Catalysis Letters
https://doi.org/10.1007/s10562-018-2507-0

Selective Production of Terminally Unsaturated Methyl Esters from Lactones Over Metal Oxide Catalysts

Zachary J. Brentzel[1] · **Madelyn R. Ball**[1] · **James A. Dumesic**[1]

Received: 12 June 2018 / Accepted: 25 July 2018

Abstract

Metal oxide catalysts were studied for their selectivity for the production of a terminally unsaturated methyl ester, methyl 5-hexenoate (M5H), from a 6 carbon, 6-membered ring lactone, δ-hexalactone (DHL). A 15 wt% Cs/SiO_2 catalyst had a selectivity of 55% to M5H. This selectivity was the highest of the metal oxide catalysts studied, which were Cs/SiO_2, MgO, SrO, CeO_2, ZrO_2, Ta_2O_5, $MgAl_2O_4$, and a Mg–Zr mixed oxide. The Cs/SiO_2 catalyst was utilized for the ring-opening of γ-valerolactone (GVL), a 5 carbon, 5-membered ring lactone. The catalyst was 88% selective to the terminally unsaturated methyl ester, methyl 4-pentenoate (M4P). Weight hourly space velocity studies determined that the unsaturated ester distributions remained constant and no C=C double bond isomerization occurred. Liquid phase transesterification reactions with DHL and methanol and nuclear magnetic resonance spectroscopy confirmed that DHL undergoes ring-opening transesterification to produce an ω-1 hydroxy methyl ester, methyl 5-hydroxyhexanoate (M5HH). Liquid phase transesterification reactions and thermochemistry calculations established that the equilibrium for GVL transesterification with methanol was favored towards the ring-closed lactone instead of the ring-opened hydroxy ester because of the decreased ring strain of GVL compared to DHL. The difference in terminally unsaturated methyl ester selectivity between GVL and DHL manifests from the difference in ring-strain energy. DHL passes through the M5HH intermediate as a result of greater ring strain, while the production of M4P from GVL most likely occurs through a direct, concerted mechanism.

Graphical Abstract

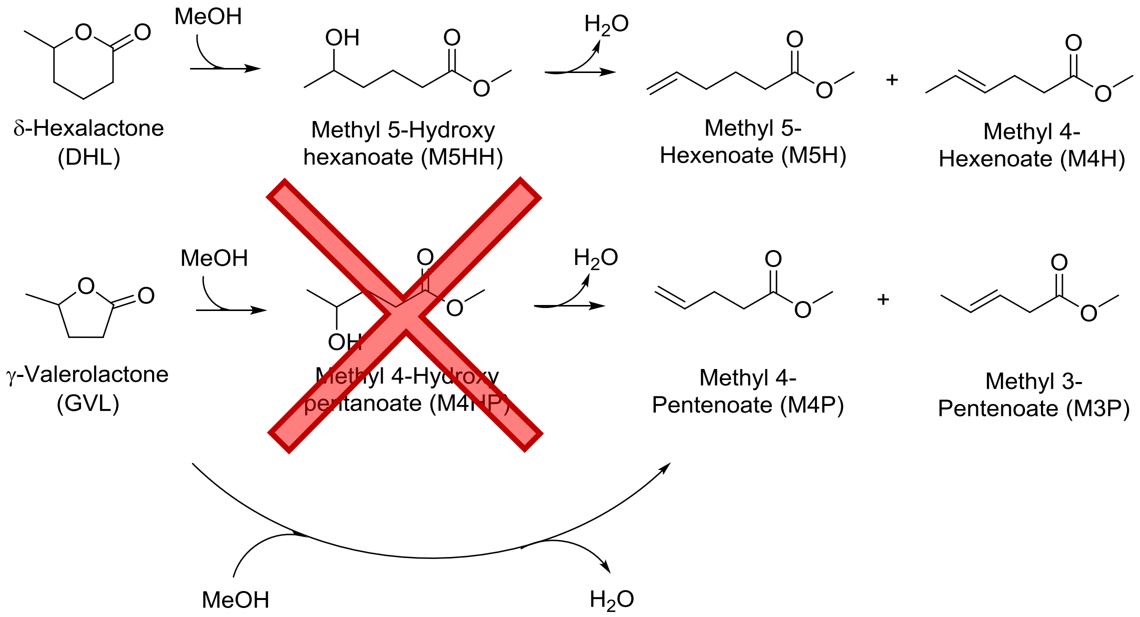

Extended author information available on the last page of the article

Keywords Biorenewable chemicals · Heterogeneous catalysis · Metal oxides · Ring-opening · Terminally unsaturated methyl esters

1 Introduction

Cyclic esters, or lactones, are a class of biorenewable molecules that can be derived from both lignocellulosic biomass and secondary metabolites of microorganisms. An emerging trend in research is to couple biological and chemical catalysis to produce high value commodity or specialty chemicals [1–4]. Biology has evolved to produce secondary metabolites with relevance to the chemical industry, such as pyrones, carboxylic acids, and bifunctional molecules [1, 5, 6].

One such biologically derived platform pyrone is triacetic acid lactone (TAL). TAL is a 2-pyrone synthesized by the polyketide pathway [1, 7, 8]. TAL is promising as a biologically-derived platform chemical for its many unique functional groups. Selective catalytic upgrading of highly oxygenated and functionalized molecules becomes easier when there are fewer repeated moieties. Prior studies have demonstrated the wide array of products that can be synthesized from TAL [9]. An initial decarboxylation of TAL leads to acetylacetone. The remainder of the products require at least one C=C hydrogenation of the inner ring to synthesize downstream products. These products include sorbic acid, parasorbic acid, pentadiene, and hexalactones.

γ-Valerolactone (GVL) is the most commonly synthesized lactone from lignocellulosic biomass. GVL is synthesized from cellulose-derived levulinic acid [10, 11]. GVL has found applications as a platform molecule for both fuels and chemicals [12]. GVL also has potential use as a green, polar aprotic solvent [13, 14].

Lactones are a key starting point to synthesize downstream products, such as unsaturated acids, hydroxy acids, or olefins [15–17]. Frequently, these lactones are required to be ring-opened. Homogeneous or heterogeneous acid catalysts will form the carbocation and yield internally unsaturated carboxylic acids, such as sorbic acid or pentenoic acids [9]. Sorbic acid is used as a food grade preservative and has annual production volumes of 65 kt/year [18]. Pentenoic acids have more limited uses industrially but find uses in synthetic cheeses.

The objective of our work is to elucidate the performance of heterogeneous catalysts to selectively produce terminally unsaturated acids or esters from biologically-derived lactones. Both homo- and hetero- α,ω-functionalized molecules have found extensive use in industry. Some of the largest volume α,ω-functionalized molecules synthesized commercially are α,ω-diols [19, 20], α,ω-carboxylic acids [21], α,ω-amines [22]. Ethylene glycol, 1,4-butanediol, and 1,6-hexanediol are the largest volume α,ω-diols produced commercially today. All three diols are used in the synthesis of polyesters, plasticizers, polyurethanes, and resins [19]. Synthesizing terminally unsaturated acids or esters is a promising lactone upgrading route, since the resulting double bond can be functionalized by a variety of reactions, such as hydroformylation, hydroamination, hydrocyanation, hydration, and hydroacylation [23].

In the present work, we study the selectivity for the ring-opening of δ-hexalactone (DHL) and GVL towards their respective methyl unsaturated esters. Various heterogeneous base catalysts were studied, including catalysts synthesized from alkali acetate that have been previously demonstrated to selectively produce terminally unsaturated esters [24]. The Cs/SiO_2 catalyst was the most selective of the catalysts studied for the production of terminally unsaturated esters. Nuclear magnetic resonance (NMR) spectroscopy, density functional theory (DFT), and probe alcohol dehydration reactions were used to elucidate the differences in terminally unsaturated ester selectivity between DHL and GVL.

2 Experimental Details

2.1 Catalysts

Commercial magnesium oxide (MgO) (Aldrich, 99.99%), strontium oxide (SrO) (Aldrich, 99.9%), cerium(IV) oxide (CeO_2) (Aldrich, ≥ 99%), tantalum(V) oxide (Ta_2O_5) (Aldrich, 99.99%), and magnesium aluminate ($MgAl_2O_4$) (Aldrich, spinel nanopowder) were used as purchased and in situ pretreated at 673 K in flowing He (Airgas, industrial grade) for 30 min prior to reaction.

The 15% Cs/SiO_2 catalyst was prepared by incipient wetness impregnation. The appropriate mass of cesium acetate, CH_3COOCs, (Sigma, ≥ 99.99%) was dissolved in deionized water (Millipore Milli-Q grade, 18 MΩ) and added dropwise to silica gel SiO_2 (Davisil Grade 646). The catalyst was calcined under flowing air (Airgas, medical grade). The temperature was held at 393 K (1.6 K/min) for 4 h and then 723 K (2.8 K/min) for 16 h.

The zirconium dioxide (ZrO_2) catalyst was synthesized by precipitation, based on methods from Serrano Ruiz et al. [25] $ZrO(NO_3)_2$ (Aldrich) was precipitated with NH_4OH (Aldrich). NH_4OH was added to maintain a pH of 10. The resulting slurry was stirred for 65 h. The filtered precipitates were calcined in flowing air (Airgas, medical grade) for 4 h at 723 K.

The MgO/ZrO_x catalyst was prepared by precipitation of $Mg(NO_3)_2 \cdot 6H_2O$ and $ZrOCl_2 \cdot 6H_2O$ with NaOH (Aldrich)

[26]. The molar ratio of $Mg(NO_3)_2{\cdot}6H_2O$ to $ZrOCl_2{\cdot}6H_2O$ was 10.9. NaOH was added to maintain a pH of 10. The filtered precipitates were calcined in flowing air (Airgas, medical grade) for 4 h at 873 K.

All catalysts were pre-treated in situ in flowing He (Airgas, industrial grade) at 673 K for 30 min prior to reaction.

2.2 Carbon Dioxide Temperature Programmed Desorption (TPD)

130 mg of the 15% Cs/SiO_2 catalyst was loaded into a fritted quartz tube and then into a temperature controlled (Love Controls) tube furnace. Vapor phase effluent was continuously sampled by a mass spectrometer (Pfeiffer Vacuum, Onmistar). The catalyst was first purged with He for 15 min at room temperature (Airgas, UHP). The catalyst was then pretreated in flowing He (Airgas, UHP) at 673 K for 30 min. The furnace was cooled and held at 298 K. CO_2 was adsorbed on the catalyst at 298 K from a 5% CO_2/N_2 (Airgas) flow for 30 min. Then, UHP He was passed over the catalyst at 298 K for 1 h to remove weakly adsorbed CO_2. After stabilizing the mass spectrometer signal, the sample was heated to 973 K (10 K/min). The reported base site densities are calculated from the CO_2 signal.

2.3 Scanning Transmission Electron Microscopy (STEM)

A FEI Titan STEM with Cs probe aberration corrector operated at 200 kV with spatial resolution <0.1 nm was used for STEM studies. Images were collected using high-angle annular dark-field (HAADF) mode, with HAADF detector angle ranging from 54 to 270 mrad, probe convergence angle of 24.5 mrad, and probe current of approximately 25 pA. Energy dispersive X-ray spectroscopy (EDS) data were collected using the same microscope with an EDAX SiLi Detector. Catalyst samples were suspended in ethanol and then dropped on a holey carbon Cu TEM grid.

2.4 Vapor Phase Ring-Opening Reactions

The vapor phase ring-opening and dehydration studies were performed in a fixed bed catalytic reactor in an up-flow configuration at 598 K and 3.5 atm. The catalyst to be studied was loaded into a 1/4" OD stainless steel tube and secured in place by alternating layers of quartz wool (Grace) and granular silicon dioxide (Sigma, 99.9%, 4–20 mesh). The silicon dioxide was used to decrease void volume and increase heat transfer. The quartz wool layers served as a buffer between the catalyst and silicon dioxide layers. The tube was secured in a furnace comprised of aluminum blocks, heating tape (Briskheat, 135 W), and insulation. The vapor phase reactor effluent was passed through an ice bath condenser. Liquid samples were collected from the condensed effluent every 2–8 h. The vapor phase was sampled via online gas chromatography (Shimadzu GC2010 equipped with a flame ionization detector (FID) and a RT-Q-Bond column). Liquid samples were analyzed by gas chromatography (Shimadzu GC2010 equipped with a FID and a DB-5MS capillary column).

The catalysts were pretreated in flowing He (Airgas, industrial grade) at 673 K for 1 h prior to the reaction. The reactor was then cooled to a reaction temperature of 598 K. The flowing He was then used as a sweep gas at the effluent of the reactor. The liquid feeds, either 50 wt% GVL (Sigma, $\geq 99\%$) in methanol (Fisher Chemical, $\geq 99.9\%$), 50 wt% DHL in methanol, neat 1-octanol (Sigma-Aldrich, $\geq 99\%$), or neat 2-octanol (Sigma-Aldrich, $\geq 99\%$), were supplied to the reactor via high performance liquid chromatography (HPLC) pump (Lab Alliance Series 1).

2.5 Liquid Phase Transesterification Reactions

The liquid phase transesterification reactions were performed at room temperature in thick walled glass reactors (Alltech, 10 mL) with magnetic stir bars. Feed solutions of 1.5 g each of lactone and methanol (Fisher Chemical, $\geq 99.9\%$) were loaded into the glass reactors. The feeds from each reaction were collected and analyzed by gas chromatography (Shimadzu GC2010 equipped with a FID and a DB-5MS capillary column). 0.01 g of concentrated sulfuric acid (Sigma-Aldrich, 95–98%) was then added to each reactor. The reactors were stirred at room temperature for 72 h and sampled every 24 h. The reactor samples were neutralized and analyzed by gas chromatography.

2.6 Nuclear Magnetic Resonance (NMR) Spectroscopy

Two samples were analyzed by NMR spectroscopy. The first sample was a 50 wt% DHL (Alfa Aesar, 98%) in deuterated dimethyl sulfoxide (DMSO-d6) (Aldrich, $\geq 99.9\%$ atomic percentage deuterium, contains 1% (v/v) TMS) solution. The second sample was the liquid phase transesterification product of 50 wt% DHL in methanol with 25 mM of sulfuric acid. The reaction product mixture was combined with 50 wt% DMSO-d6 before NMR analysis. One-half a gram of each solution was added to an NMR tube (Wilmad, 5 mm borosilicate glass).

NMR experiments were performed on a Bruker Avance-III 500 MHz spectrometer with a DCH cryoprobe. All spectra were collect at 297 K. The ^2H signal from DMSO-d6 was used as the field-frequency lock. The magnetic field shimming was performed on the ^2H solvent signals. ^1H and ^{13}C chemical shifts were referenced against the tetramethylsilane (TMS) peak in the DMSO-d6 solvent. ^1H experiments were performed with a Bruker standard 1D pulse sequence, ‘zg30’. The inter-scan relaxation delay, sweep width, acquisition time, and number of scans were 2 s, 20 ppm centered at 10 ppm, 3.3 s, and 8 scans, respectively. ^{13}C spectra were collected with a ^{1}H decoupled pulse sequence, ‘zgpg30’. The inter-scan relaxation delay, sweep width, acquisition time, and number of scans were 2 s, 284 ppm centered at 110 ppm, 2 s, and 32 scans, respectively. The ^{13}C distortionless enhancement of polarization transfer with a 135° angle for the φ_3 pulse (DEPT-135) spectrum was collected with a Bruker standard pulse sequence, ‘deptsp135’. The inter-scan relaxation delay, sweep width, acquisition time, and number of scans were 2 s, 284 ppm centered at 110 ppm, 1 s, and 32 scans, respectively. 2D ^{1}H–^{1}H homonuclear correlation spectroscopy (COSY) spectra were collected with a Bruker standard pulse sequence, ‘cosygp45’. The scan had the following parameters: 16 ppm sweep width in F2 (^{1}H), centered at 4.5 ppm, acquiring 2048 data points, 16 ppm sweep width in F1 (^{1}H), centered at 4.5 ppm, acquiring 256 increments, 2 scans per increment, and a 2 s relaxation delay. 2D ^{1}H–^{13}C heteronuclear single quantum coherence (HSQC) spectra were collected with a Bruker standard pulse sequence, ‘hsqcetgp’. The scan had the following parameters: 12 ppm sweep width in F2 (^{1}H), centered at 4.7 ppm, acquiring 2048 data points, 180 ppm sweep width in F1 (^{13}C), centered at 85 ppm, acquiring 256 increments, 2 scans per increment, and a 2 s relaxation delay. 2D ^{1}H–^{13}C heteronuclear multiple-bond correlation spectroscopy (HMBC) spectra were collected with a standard pulse sequence, ‘hmbcetgp’. The scan had the following parameters: 12 ppm sweep width in F2 (^{1}H), centered at 4.7 ppm, acquiring 4096 data points, 240 ppm sweep width in F1 (^{13}C), centered at 110 ppm, acquiring 256 increments, 4 scans per increment, an 8 Hz long range coupling constant, and a 2 s relaxation delay.

2.7 Density Functional Theory (DFT) Calculations

Gaussian 09 software was used for DFT calculations to estimate the gas phase thermochemistry for the ring-opening transesterification of DHL and GVL with methanol. Geometry optimizations and frequency calculations were performed using B3LYP/6-311+G(2d,p).

3 Results and Discussion

The proposed reaction networks for the production of terminally unsaturated methyl esters from DHL and GVL are shown in Fig. 1. Eight catalysts were studied for their selectivity to the production of methyl 5-hexenoate (M5H) from DHL, shown in Table 1. When using a commonly studied heterogeneous base, MgO, the reaction had a mass balance of only 70%, with 50% of the remaining carbon converted to unknown products. The reactor effluent contained solid particles, indicative of polymer formation. Additionally, the distribution of methyl 4-hexenoate (M4H) to M5H unsaturated esters was nearly 2:1. There was no selectivity to either of the two other most common products,

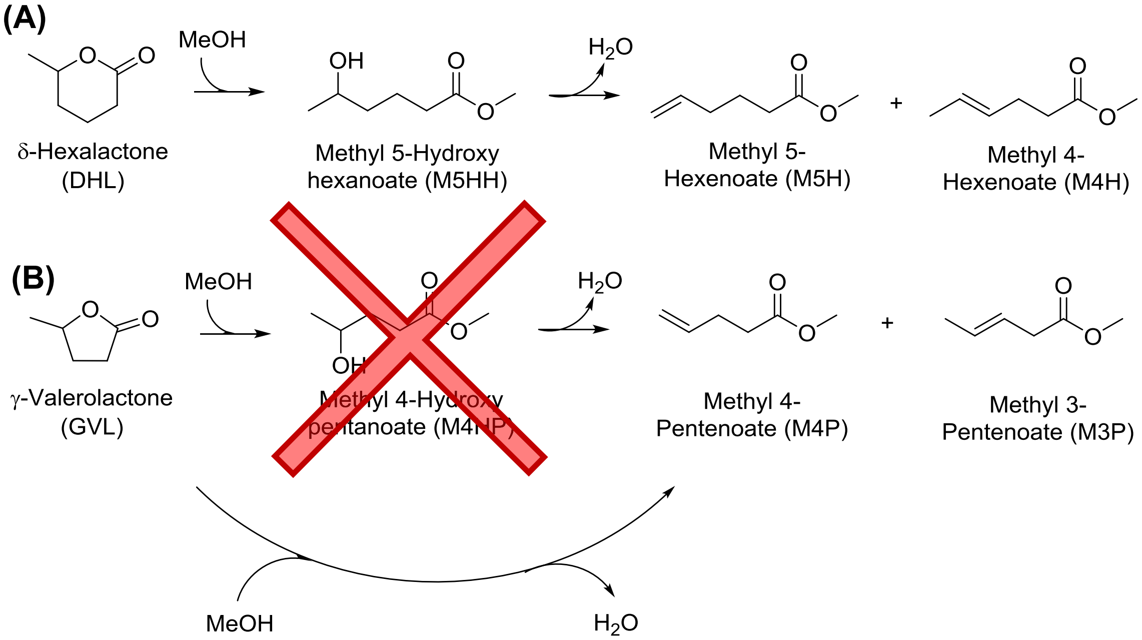

Fig. 1 Proposed reaction pathways for the production of **a** methyl hexenoates from of DHL and methanol and **b** methyl pentenoates from GVL and methanol

Table 1 Selectivity for the vapor phase lactone ring-opening of DHL with a methanol co-feed for heterogeneous catalysts

Catalyst	Conversion (%)	Methyl 5-hexenoate (M5H) selectivity (mol%)	Methyl 4-hexenoate (M4H) selectivity (mol%)	Selectivity to methyl 5-hydroxyhexanoate (M5HH) (mol%)	Selectivity to cyclohexenone (mol%)
MgO	93	18	32	0	0
SrO	10	3	3	94	0
CeO_2	60	24	26	54	0
MgZr	11	2	1	94	2
ZrO_2	32	22	7	23	22
$MgAl_2O_4$	18	1	1	94	0
Ta_2O_5	11	6	3	64	0
15% Cs/SiO_2	15	45	19	35	0
15% Cs/SiO_2[a]	77	55	30	15	0
SiO_2	12	0	0	100	0

The reactions were carried out at 598 K, 3.5 bar, and 50 wt% DHL in methanol feed

[a] The second entry for 15% Cs/SiO_2 provides results from a reaction carried out at longer space time

methyl 5-hydroxyhexanoate (M5HH) and cyclohexenone. Reactions with the remainder of the catalysts resulted in selectivities of at least 23% to M5HH. Zr-containing catalysts, both MgZr and ZrO_2, had selectivities between 2 and 22% to cyclohexenone. No other catalysts produced cyclohexenone. We hypothesize that the production of cyclohexenone is a function of the amphoteric nature of the Zr catalysts [27]. MgZr and ZrO_2 also had the largest ratio of M5H to M4H. Cs/SiO_2 had 64% selectivity to the unsaturated esters and 35% to M5HH at 15% conversion. Cs/SiO_2 had 45% selectivity to M5H. Ta_2O_5 had 62% distribution to M5H, but mainly produced M5HH, while SrO, CeO_2, and $MgAl_2O_4$ were more selective to the internal unsaturated ester, M4H, than the terminal unsaturated ester, M5H.

The Cs-containing catalyst was used for further study of ring-opening of DHL and GVL since it had the highest selectivity and yield to M5H. The maximum yield to the terminal unsaturated ester was studied for each lactone. There was 88% selectivity to methyl 4-pentenoate (M4P) and 6% selectivity to methyl 3-pentenoate (M3P) at 63% conversion of GVL, which is the equilibrium conversion. However, there was only 55% selectivity to M5H and 30% selectivity to M4H at 77% conversion from DHL, which is the equilibrium conversion.

The synthesis of Cs/SiO_2 by wetness impregnation of silica with cesium acetate and subsequent calcination results in cesium carbonate and cesium oxide nanoparticles supported on the silica support [24]. Cs nanoparticles can be seen in the scanning transmission electron micrographs in Fig. 2. EDS was used to confirm that these were Cs-containing particles. The cesium nanoparticles had particle sizes ranging from 10 to 85 nm. Cesium oxide is a heterogeneous base, and CO_2 TPD was used to quantify the base site density. The catalyst had a base site density of 7.4 μmol/g, and the CO_2 began desorbing at 30 °C and had completely desorbed by 200 °C, which is indicative of a weak base. A weaker base is preferred for a selective lactone ring opening because stronger bases, such as MgO, had poorer selectivity to the terminally unsaturated methyl esters.

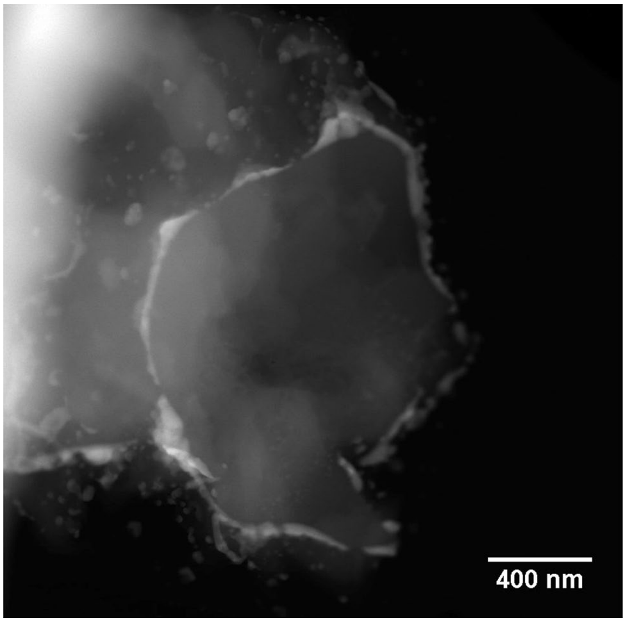

Fig. 2 Scanning transmission micrograph of 15% Cs/SiO_2 catalyst showing 10–85 nm cesium particles

Weight hourly space velocity studies were performed to determine if the differences in selectivities to the terminal unsaturated esters for the C5 and C6 lactones were a function of C=C double bond isomerization, as shown in Fig. 3. Neither the hexenoate nor pentenoate esters isomerized with increasing space time. The distribution to M4P was 94%

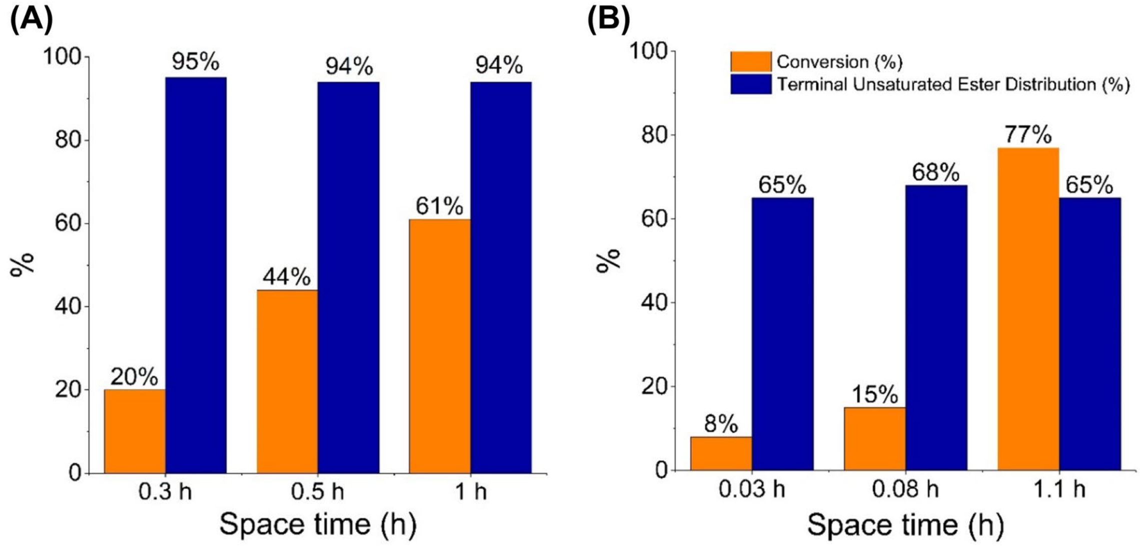

Fig. 3 The distribution of terminal unsaturated esters to all unsaturated ester production for **a** GVL and **b** DHL over a 15 wt% Cs/SiO$_2$ catalyst. The reactions were carried out at 598 K, 3.5 bar, and 50 wt% lactone in methanol feed. The data correspond to samples taken at steady state. Units of space time are h g$_{cat}$/g$_{lactone}$

from 20% conversion up to 60% conversion. The distribution to M5H remained at 65% from 8% conversion to 77% conversion.

Ring-opening of GVL and DHL occur through separate mechanisms over the Cs/SiO$_2$ catalyst since C=C double bond isomerization does not occur and there is a 30% difference in the distribution to the terminal unsaturated esters. A reactor absent of a catalyst and only packed with inert, high purity fused silicon dioxide granules was studied to determine if there were any differences in conversion or selectivity for the C5 and C6 lactones. This blank reaction demonstrated that there was 12% conversion to the transesterification product, methyl 5-hydroxyhexanoate (M5HH), for the DHL feed. The same reaction performed with GVL only yielded < 1% to its transesterification product, methyl 4-hydroxypentanoate (M4HP).

Further studies were conducted in the liquid phase to determine the extent of transesterification between the lactones and their ring-opened ω-1 hydroxy methyl esters. The 50 wt% lactone feeds in methanol were prepared and allowed to equilibrate at room temperature for 1 week. Analysis of each mixture after that week showed that the GVL and methanol mixture had not undergone conversion, while the DHL and methanol feed had reached 50% yield to the hydroxy ester. A subsequent experiment was conducted to study the equilibrium transesterification conversion at room temperature by adding a small amount of acid. Each mixture was acidified to 25 mM with 95% H$_2$SO$_4$, stirred at room temperature for 72 h, and sampled every 24 h. The mixtures reached equilibrium conversion by 24 h. The yields to the respective hydroxy esters are shown in Table 2. DHL was converted by 92% to M5HH, while GVL was converted by only 21% to M4HP.

Table 2 Conversion to the respective ω-1 hydroxy ester for two 5-membered ring and two 6-membered ring lactones

Molecule	Equilibrium conversion to hydroxy ester (%)	
	298 K, liquid phase	598 K, 3.5 bar, vapor phase
γ-Valerolactone (GVL)	21	< 1
γ-Hexalactone (GHL)	12	Not run
δ-Nonalactone (DNL)	87	Not run
δ-Hexalactone (DHL)	92	12

The vapor phase reactions were carried out at 598 K, 3.5 bar, and 50 wt% DHL in methanol feed with only SiO$_2$ granules in the reactor. The liquid phase reactions were conducted at 298 K for 72 h with 5 g of 50 wt% lactone in MeOH with 1 drop of 70 wt% HCl

To study the effects of lactone ring-size further, we performed the same experiment with γ-hexalactone (GHL) and δ-nonalactone (DNL). GHL is a 5-membered lactone ring with an ethyl group substituent, and DNL is a 6-membered lactone ring with a butyl functional group, shown in Fig. 4. Lactone ring-size is the determining factor in the equilibrium conversion to the respective ω-1 hydroxy esters. The 6-carbon GHL has 12% equilibrium conversion to its transesterified product, methyl 4-hydroxyhexanoate (M4HH). That value is closest to the 5-membered lactone, GVL, and not the 6-membered ring, DHL. The 9-carbon, 6-membered ring DNL has 87% equilibrium conversion to its hydroxy

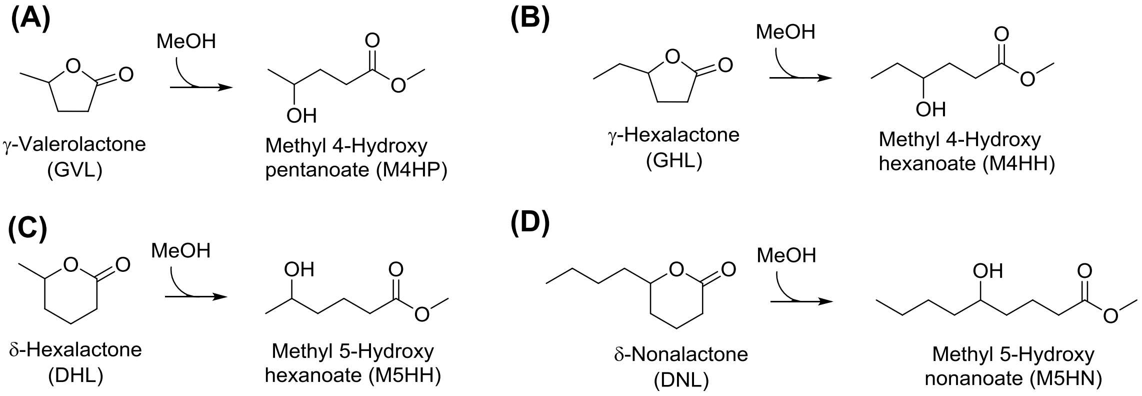

Fig. 4 Transesterification of **a** GVL to M4HP, **b** GHL to M4HH, **c** DHL to M5HH, and **d** DNL to M5HN

ester, methyl 5-hydroxynonanoate (M5HN). This value is comparable to the 6-membered ring, DHL, which has 92% conversion. Liquid phase transesterification of lactones with methanol is predominantly a function of ring size and not carbon number. Only DHL and GVL were studied for their conversion to ω-1 hydroxy esters under vapor phase reaction conditions over high purity silicon dioxide granuales. Although, the conversion in the vapor phase is not necessarily equilibrium conversion, the same trend was observed. The 6-membered ring DHL underwent 12% conversion to the M5HH, while GVL underwent < 1% conversion to M4HP.

The hypothesized reason for such large discrepancies between equilibrium conversion to the respective transesterified hydroxy esters between the 5- and 6-membered ring lactones is the ring strain. Calorimetry experiments have determined that 5-membered ring, GVL, has 30.5 kJ/mol of ring strain, while a 6-membered lactone ring, δ-valerolactone (DVL) has 39.7 kJ/mol [28]. Stedjan et al. have performed DFT calculations and found that the difference in ring strain energy between 5- and 6-membered lactone rings was 9.6 kJ/mol, similar to what was determined experimentally [29]. Additional thermochemistry calculations were performed using Gaussian 09 DFT software to predict the gas phase energies for all of the reactants and products. The Gibbs free energy change at 298 K for the transesterification of the two 5-membered ring lactones, GVL and GHL, was 19 kJ/mol, while the free energy change for the two 6-membered ring lactones, DHL and DNL, was 2 kJ/mol. This trend corresponds with the trend observed for the liquid phase equilibrium conversion of the lactones to their respective hydroxy esters (Table 3).

Table 3 Thermochemistry values for the transesterification of lactones and methanol to their respective ω-1 hydroxy methyl esters at 298 K

Reactant	ΔH (kJ/mol)	ΔS (kJ/mol/K)	ΔG (kJ/mol)
γ-Valerolactone (GVL)	− 19.1	−0.13	19.4
γ-Hexalactone (GHL)	− 19.5	−0.13	18.8
δ-Nonalactone (DNL)	− 36.7	−0.13	1.8
δ-Hexalactone (DHL)	− 35.1	−0.12	2.1

Energies were estimated using B3LYP/6-311+G(2d,p) with Gaussian 09 DFT (DFT) software

NMR spectroscopy was used to probe the structure of the ring-opened, transesterified product, M5HH. Carbon and hydrogen peaks for DHL were also identified and confirmed. Standard ^{1}H, standard ^{13}C, ^{13}C DEPT-135, 2D ^{1}H–^{1}H COSY, 2D ^{1}H–^{13}C HSQC, and 2D ^{1}H–^{13}C HMBC scans were performed for both 50 wt% DHL in DMSO-d6 and the 50:50 w/w DHL:MeOH solution with 25 mM of sulfuric acid diluted in 50 wt% DMSO-d6. The ^{1}H decoupled ^{13}C NMR spectra for both DHL and M5HH are shown in Fig. 5. The peaks were assigned by comparing the ^{13}C DEPT-135, 2D ^{1}H–^{1}H COSY, 2D ^{1}H–^{13}C HSQC, and 2D ^{1}H–^{13}C HMBC spectra. The ^{13}C DEPT-135 spectrum for M5HH, shown in Fig. 6, confirms the proper orientation of $–CH_2$ peaks as negative, while the –CH and $–CH_3$ peaks are positive. The key evidence to distinguish between the ring-closed lactone and the ring-opened hydroxy ester is ascertained with 2D ^{1}H–^{13}C HMBC. This technique is used to detect proton-carbon correlation over a 2–3 bond range. HMBC has been successfully applied to confirm lactone structures through the cyclic heteroatom previously in literature [30–33]. HMBC results for DHL demonstrate that the ester carbon, denoted 6, is correlated with protons on carbons 1, 4, and 5, as shown in Fig. 7a. There was a smaller peak corresponding to the correlation with protons on carbon 2. The protons on carbon 3 were not coupled with carbon 6 with the coupling constant of 8 Hz. The HMBC spectrum of M5HH proved that carbon 6 was only correlated with protons on carbons 4, 5, and 7, as shown in Fig. 7b. The lack of correlation to protons on carbons 1, 2, or 3 confirm the presence of a ring-opened species.

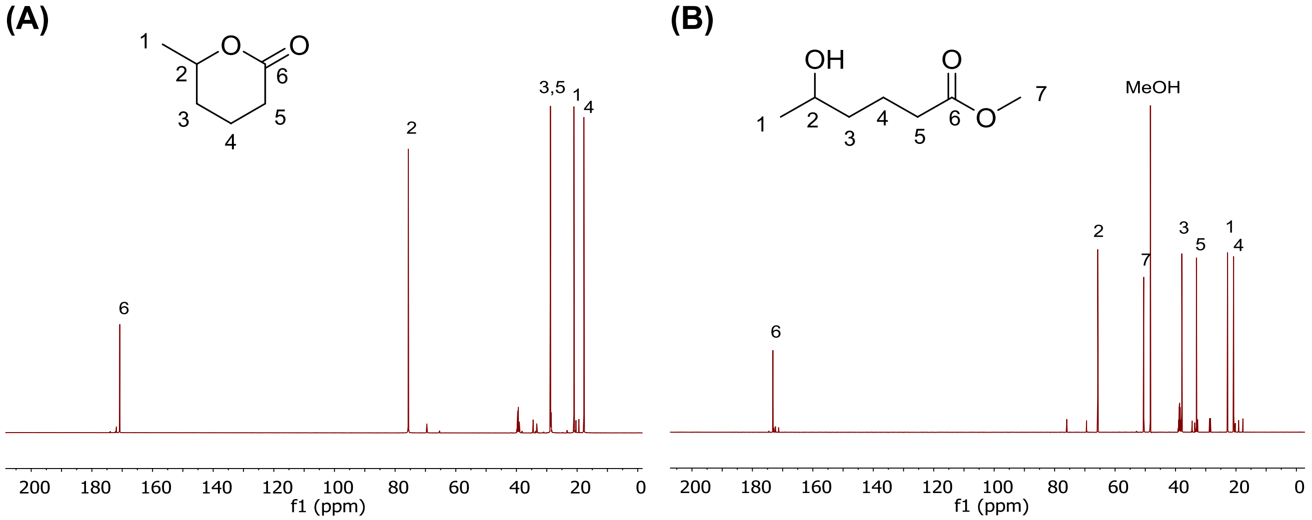

Fig. 5 ^1H decoupled ^{13}C NMR spectra and peak identification of **a** 50 wt% DHL in DMSO-d8 and **b** reaction product from 50:50 (w/w) DHL:MeOH with 25 mM concentrated sulfuric acid in 50 wt% in DMSO-d8

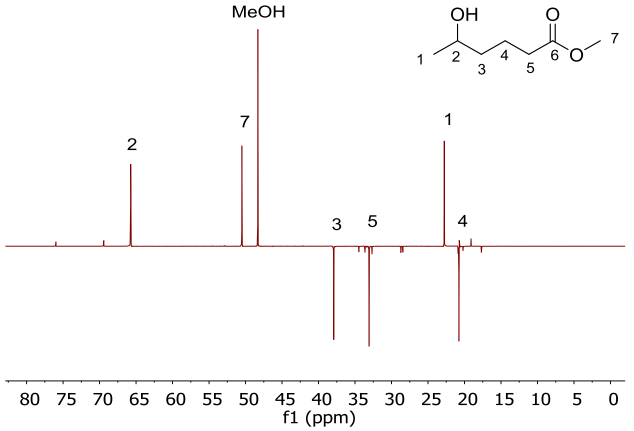

Fig. 6 ^{13}C DEPT-135 NMR spectrum and peak identification of the reaction product from 50:50 (w/w) DHL:MeOH with 0.01 g concentrated sulfuric acid in 50 wt% in DMSO-d8. –CH_2 peaks are negative. –CH and –CH_3 peaks are positive

Since DHL undergoes homogenous transesterification to M5HH under reaction conditions, we studied the selectivity of alcohol dehydration to mimic the functionality of the ω-1 hydroxyl moiety of M5HH. 1- and 2-Octanol were chosen as the probe alcohol molecules. Table 4 provides the results from the alcohol dehydration studies. The dehydration of 1-octanol was performed to verify the negligible C=C double bond isomerization on the resulting alkene that had previously been observed for the unsaturated esters. 1-Octene is the only primary product, and therefore, the formation of 2-octene occurs as a secondary reaction through double bond isomerization. At 8% conversion over Cs/SiO_2, 1-octanol dehydration was 99% selective to 1-octene. The selectivity to *trans*-2-octene was only 1%, and there was no production of *cis*-2-octene. Therefore, there was negligible C=C double bond isomerization for the linear alpha olefin. Dehydration of 2-octanol can produce either 1- or 2-octenes as primary products. Since we have demonstrated that there is no C=C double bond isomerization, the selectivity to both of these products results from the primary reaction of dehydration. The selectivities for the dehydration of 2-octanol to 1-octene, *trans*-2-octene, and *cis*-2-octene were 75, 10, and 15%, respectively. These distributions correlate well with those obtained from the production of methyl hexenoates from DHL. At equilibrium conversion of DHL, the distribution to the terminal unsaturated ester is 65%. The selectivities and lack of C=C double bond isomerization achieved in the probe alcohol dehydration studies provide further evidence that the 6-membered lactone ring, DHL, undergoes a ring opening transesterification followed by dehydration, as shown in Fig. 1. The differences in terminal unsaturated ester selectivity, unfavorable transesterification thermodynamics, and steric hindrance of methoxide addition to GVL suggest that the 5-membered lactone ring undergoes a direct, concerted ring-opening mechanism. This behavior allows for higher selectivity to the terminal unsaturated bond.

4 Conclusions

We have demonstrated that Cs/SiO_2 catalysts display > 55% selectivity to M5H from DHL and 88% selectivity to M4P from GVL. The difference in selectivity manifests from the larger degree of ring strain in the C6 lactone compared to the C5 lactone. NMR experiments and liquid phase transesterification reactions have determined that the uncatalyzed product observed from the vapor phase

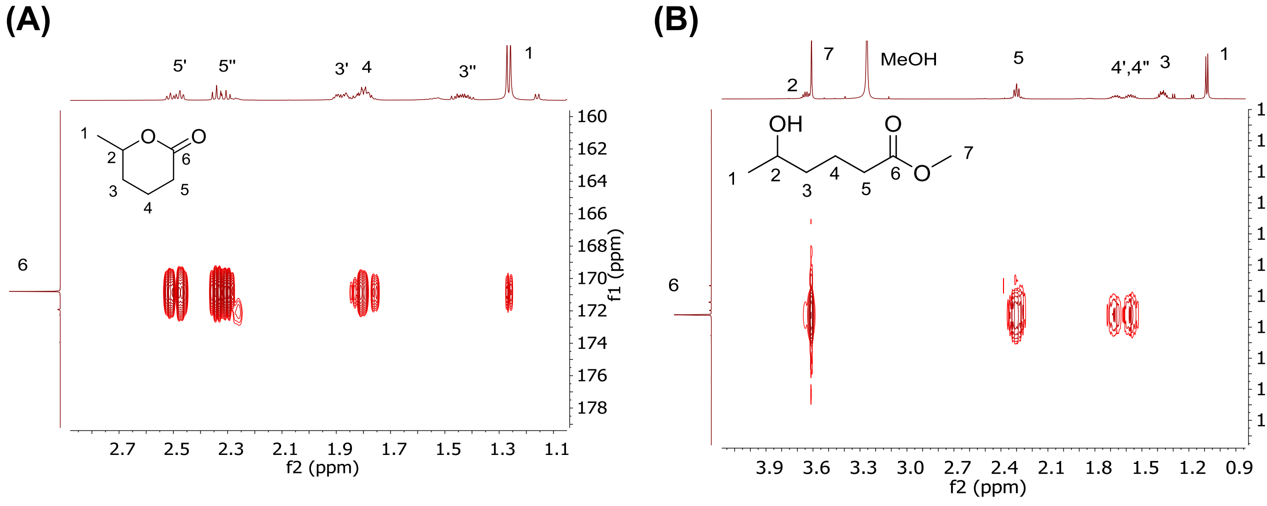

Fig. 7 Heteronuclear multiple-bond correlation spectroscopy (HMBC) NMR spectra for the ester carbon, number 6, for **a** 50 wt% DHL in DMSO-d8 and **b** reaction product from 50:50 (w/w) DHL:MeOH with 25 mM concentrated sulfuric acid in 50 wt% in DMSO-d8

Table 4 Conversion and selectivity of 1- and 2-octanol over Cs/SiO_2

Feed	Conversion (%)	Octene distribution (%)		
		1	*Trans*-2-	*Cis*-2-
1-Octanol	8	99	1	0
2-Octanol	5	75	10	15

The reactions were carried out at 598 K, 3.5 bar, and neat octanol

reaction of methanol with DHL is the ring-opened, transesterification product, M5HH. DFT calculations and liquid phase transesterification reactions show that the equilibrium distribution for the transesterified ω-1 hydroxy methyl ester is significantly greater for 6-membered lactone rings compared with 5-membered rings. Comparable molar ratios of terminal to internal unsaturated C=C bonds from dehydrations of a probe secondary alcohol, 2-octanol, suggests that the mechanism for production of M5H passes through the M5HH intermediate, while negligible conversion of GVL to M4HP indicates that GVL undergoes a direct, concerted mechanism to M4P.

Acknowledgements This material is based upon work supported by the National Science Foundation Engineering Research Center for Biorenewable Chemicals (CBiRC), under Award Number EEC-0813570. The authors would like to thank the Magnetic Resonance Facility in the Chemistry Department of the University of Wisconsin-Madison for use of the Bruker Avance III 500 gifted by Paul J. Bender. The use of facilities supported by the Wisconsin Materials Research Science and Engineering Center is also acknowledged (DMR-1121288). We thank Leo Manzer and Thomas Schwartz for helpful discussions about lactone ring-opening. We thank Heike Hofstetter for discussions about NMR analyses. Any opinions, findings, and conclusions or recommendations expressed in this material are those of the authors and do not necessarily reflect the views of the National Science Foundation.

References

1. Nikolau BJ, Perera MADN, Brachova L, Shanks B (2008) Plant J 54:536–545
2. Shanks BH (2007) ACS Chem Biol 2:533–535
3. Schwartz TJ, O'Neill BJ, Shanks BH, Dumesic JA (2014) ACS Catal 4:2060–2069
4. Schwartz TJ, Shanks BH, Dumesic JA (2016) Curr Opin Biotechnol 38:54–62
5. Bowen CH, Bonin J, Kogler A, Barba-Ostria C, Zhang F (2016) ACS Synth Biol 5:200–206
6. Dellomonaco C, Clomburg JM, Miller EN, Gonzalez R (2011) Nature 476:355–359
7. Cardenas J, Da Silva NA (2014) Metab Eng 25:194–203
8. Jez JM, Bowman ME, Noel JP (2002) Proc Natl Acad Sci USA 99:5319–5324
9. Chia M, Schwartz TJ, Shanks BH, Dumesic JA (2012) Green Chem 14:1850
10. Alonso DM, Bond JQ, Dumesic JA (2010) Green Chem 12:1493
11. Wettstein SG, Alonso DM, Chong Y, Dumesic JA (2012) Energy Environ Sci 5:8199
12. Horváth IT, Mehdi H, Fábos V, Boda L, Mika LT (2008) Green Chem 10:238–242
13. Mellmer MA, Martin Alonso D, Luterbacher JS, Gallo JMR, Dumesic JA (2014) Green Chem 16:4659–4662
14. Mellmer MA, Sener C, Gallo JMR, Luterbacher JS, Alonso DM, Dumesic J (2014) Angew Chem Int Ed Engl 53:11872–11875
15. Bond JQ, Wang D, Alonso DM, Dumesic JA (2011) J Catal 281:290–299
16. Bond JQ, Alonso DM, West RM, Dumesic JA (2010) Langmuir 26:16291–16298
17. Wang D, Hakim SH, Alonso DM, Dumesic JA (2013) Chem Commun (Cambridge) 49:7040–7042
18. Dorko CL, Ford GT, Baggett MS, Behling AR, Carmen HE (2014) Kirk-Othmer encyclopedia of chemical technology. Wiley, Hoboken, pp 1–19
19. Werle P, Morawietz M, Lundmark S, Sörensen K, Karvinen E, Lehtonen J (2008) Ullmann's encyclopedia of industrial chemistry. Wiley-VCH Verlag GmbH & Co. KGaA, Weinheim

20. Market sand Markets (2014) 1,6-Hexanediol market by application (polyurethanes, coatings, acrylates, adhesives, unsaturated polyester resins, plasticizers, and others) and by geography (NA, Europe, Asia-Pacific, & ROW) - Trends and Forecasts to 2019, 2014
21. Oppenheim JP, Dickerson GL (2003) Kirk-Othmer encyclopedia of chemical technology. Wiley, Hoboken
22. Sridhar S, Carter RG (2001) Kirk-Othmer encyclopedia of chemical technology. Wiley, Hoboken
23. Beller M, Seayad J, Tillack A, Jiao H (2004) Angew Chem Int Ed Engl 43:3368–3398
24. Manzer L US6835849B2, 2004, 1.
25. Serrano-Ruiz JC, Luettich J, Sepúlveda-Escribano A, Rodríguez-Reinoso F (2006) J Catal 241:45–55
26. Aramendía MA, Boráu V, Jiménez C, Marinas A, Marinas JM, Navío JA, Ruiz JR, Urbano FJ (2004) Colloids Surf A 234:17–25
27. Ono Y, Hattori H (2011) Solid base catalysis, vol 101. Springer, Berlin
28. Brown JM, Conn AD, Pilcher G, Leito MLP, Meng-Yan Y (1989) J Chem Soc Chem Commun. https://doi.org/10.1039/C39890001817
29. Stedjan MK, Augspurger JD (2015) J Phys Org Chem 28:298–303
30. Boonphong S, Kittakoop P, Isaka M, Pittayakhajonwut D, Tanticharoen M, Thebtaranonth Y (2001) J Nat Prod 64:965–967
31. Li X, Sattler I, Lin W (2007) J Antibiot (Tokyo) 60:191–195
32. Barrow CJ (1997) J Nat Prod 60:1023–1025
33. Colmenares AJ, Durán-Patrón RM, Hernández-Galán R, Collado IG (2002) J Nat Prod 65:1724–1726

Affiliations

Zachary J. Brentzel[1] · Madelyn R. Ball[1] · James A. Dumesic[1]

✉ James A. Dumesic
jdumesic@wisc.edu

[1] Department of Chemical and Biological Engineering, University of Wisconsin-Madison, 1415 Engineering Drive, Madison, WI, USA